ARCHIVES OF ACOUSTICS
30, 3, 345–355 (2005)

DETERMINATION OF AIR-TIGHTNESS OF THE PACKAGINGS OF ELECTRONIC DEVICES BY THE THERMOACOUSTIC METHOD

M. MALIŃSKI

Technical University of Koszalin
Department of Electronics
Śniadeckich 2, 75-328 Koszalin, Poland
email: mmalin@tu.koszalin.pl

(*received October 1, 2004; accepted April 5, 2005*)

The method of determination of air-tightness of packagings based on the measurement of the thermoacoustic signals generated by transistor chips is described in this paper. This method makes possible the estimation of the radius of the hole in the packaging and, as a result, its air-tightness. In this paper the fitting of the theoretical model to experimental results is presented and discussed. Because of its simplicity and nondestructive character, the presented method can be applied in the quality control departments of the electronic industry.

Key words: air-tightness, thermoacoustics.

1. Introduction

Air-tightness of the packaging is an important parameter which must be controlled in the electronic industry works. The measuring techniques are very often troublesome because they require either high pressures and special liquids, as it is in the case of a pressure bomb, or gases as it is in the trace gas method [1, 2], or elevated temperatures and liquids [3] or low pressure and liquids [3], depending on the kind of a test. Most often these methods are time consuming and also destructive. The aim of this work was to test and estimate the threshold level of the air leaks that can be determined by the thermoacoustic technique. For the purpose of interpretation of the thermoacoustic results, the electric model of a gas transport from the packaging to the thermoacoustic cell is presented and discussed in this paper. The method of detection presented in the paper is especially useful for metal packagings TO-3, TO-18, TO-39, TO-72 of electronic devices and for the packagings of hybrid circuits. The idea of the testing method presented in this paper is based on the theory of a thermophone elaborated and published by H.D. ARNOLD and I. B. CRANDALL [4]. Thermophones were used in the past for pressure calibration of measuring microphones since it was expected that it was possible to calculate this way the absolute value of acoustic pressure in the closed chamber

and its frequency characteristics. The modern mathematical model of both the photo- and thermoacoustic effect was elaborated by A. ROSENCWAIG and A. GERSHO in 1976 [5]. The theory of the thermal-piston and mechanical-piston effects responsible for the thermoacoustic effect, used for the detection of air-tightness described in this paper, was next elaborated by H. HU *et al*. in 1999 [6]. The results of investigations of air-tightness of the plastic packaging of power transistors with a photoacoustic microscopic thermal wave method with the optical heat flux generation were presented by Z. SUSZYŃSKI in papers [7, 8]. In this method, the areas of exfoliation of the plastic encapsulant from the metal lead frames were localized. Similar method of thermal wave imaging with a thermoacoustic detection was also applied for the detection of a place of exfoliation of the packaging by A. BODERMAN in 1996 [9] and A. ROSENCWAIG and J. OPSAL in 1986 [10].

2. Theory

The flow of the mass of gas through the pipe of radius r and length L can be described by the Poiseuille Eq. (1):

$$\frac{dm}{t} = \frac{\rho \cdot \pi \cdot r^4}{\eta \cdot 8 \cdot L} \cdot dp, \tag{1}$$

where *dm* – mass of the gas, t – time of flow, ρ – density of the gas, η – viscosity of gas, L – length of the pipe or thickness of metal wall of the packaging, r – is the radius of the hole. By analogue with the Ohm law $I = V/R$, the resistance of the gas flow can be determined as:

$$R = \frac{\eta \cdot 8 \cdot L}{\pi \cdot r^4 \cdot \rho} = \frac{dp \cdot t}{dm}. \tag{2}$$

Because of the Clapeyron equation, this amount of gas *dm* flowing into the chamber of volume V causes the increase of the overpressure *dp* given by the Eq. (3).

$$dp = \frac{dm \cdot N_a \cdot k \cdot T}{M \cdot V}. \tag{3}$$

Here N_a is the Avogadro number, k – Boltzman constant, T – temperature, V – volume of the chamber, M – molar mass of the air.

Thus the heat capacity of the chamber can be determined as:

$$C_i = \frac{M \cdot V_i}{N_a \cdot k \cdot T}. \tag{4}$$

It is an analogue of the electric condenser where $V = Q/C$ and Q is the electric charge, V is the voltage and C is the capacity of the condenser.

The schematic diagram of the thermoacoustic chamber with the transistor in the metal case is presented in Fig. 1.

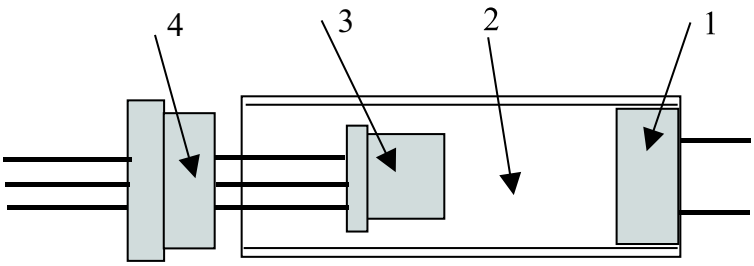

Fig. 1. A schematic diagram of the thermoacoustic chamber with a microphone. Description: 1 – microphone, 2 – thermoacoustic chamber, 3 – transistor, 4 – stopper.

The idea of the presented thermoacoustic (TA) method is based on the periodic heat generation in volume V_1 of a transistor (3) and measurement of the periodic overpressure in the volume V_2 of the thermoacoustic chamber (2), being result of the air flow from volume V_1 to V_2 through the hole in the packaging of a transistor. Frequency amplitude and phase TA characteristics bring information about the radius of the hole and in general, about the air tightness of the packaging.

Changes of the pressure in the thermoacoustic chamber can be described in the model being the electric analog of the gas flow from the volume of the transistor to the volume of the thermoacoustic chamber. In this model pressure corresponds to voltage, electric capacity to heat capacity, resistance of the mass flow to electric resistance, velocity of mass transport to electric current. The schematic diagram of the electric model describing the gas flow is presented in Fig. 2.

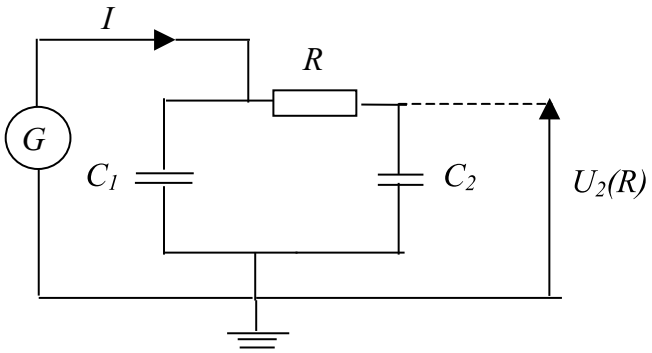

Fig. 2. An electric model of the gas flow. R is the resistance, $C_i\,(i = 1, 2)$ are capacities. G is the current generator.

The value of the voltage $U_2(R)$ is given by Eq. (5).

$$U_2(R) = \left[\frac{-i}{\omega(C_1 + C_2) + i\omega^2 C_1 C_2 R}\right] \cdot I. \tag{5}$$

The value of $U_2(R=0)$ is given by Formula (6).

$$U_2(R=0) = \left[\frac{-i}{\omega(C_1+C_2)}\right] \cdot I. \tag{6}$$

Thus the ratio of voltages is given by Formula (7). It expresses the ratio of the voltages and the corresponding pressures of the packaging exhibiting a hole, expressed by the resistance R and the open packaging ($R=0$) corresponding the case of a huge hole in the packaging.

$$\frac{U_2(R)}{U_2(0)} = \frac{\omega(C_1+C_2)}{\omega(C_1+C_2)+i\omega^2 C_1 C_2 R}. \tag{7}$$

The modulus of the ratio of the voltages (overpressures) and the phase delay of the thermoacoustic signal relative to the electric current $I$are given by Formula (8) and (9) respectively when C_i and R are given by Eqs. (2) and (4).

$$\left|\frac{U_2(r)}{U_2(0)}\right| = \frac{1}{\sqrt{1+(\omega\tau(r))^2}}, \tag{8}$$

$$\varphi = \operatorname{arctg}(-\omega\tau(r))\frac{180}{\pi}, \tag{9}$$

$$\tau(r) = \frac{\eta 8 L M V_2}{\pi \cdot r^4 \rho N_a k T (1+V_2/V_1)}, \tag{10}$$

For the computations presented below the following values of the parameters were taken:

$$\eta = 1.7\cdot 10^{-5}\,[\mathrm{Ns/m^2}], \quad L = 10^{-4}\,[\mathrm{m}], \quad M = 28\cdot 10^{-3}\,[\mathrm{kg/mole}],$$
$$V_2 = 2.5\cdot 10^{-6}\,[\mathrm{m^3}], \quad V_2/V_1 = 5, \quad r = 20\,\mu\mathrm{m}...60\,\mu\mathrm{m},$$
$$\rho = 1.3\,[\mathrm{kg/m^3}], \quad N_a = 6\cdot 10^{23}\,[\mathrm{mole^{-1}}],$$
$$T = 300\,\mathrm{K}, \quad k = 1.38\cdot 10^{-23}\,[\mathrm{J/K}].$$

The results of theoretical computations of the amplitude of the thermoacoustic (TA) signal versus the frequency of modulation are presented in Fig. 3.

The results of theoretical computations of the phase of the TA signal versus the frequency of modulation are presented in Fig. 4.

Because the calibration characteristics of the system are often not known and the TA signal depends, among others, on the thickness of a transistor chip and the quality of soldering of the chip to the lead frame [11–13], the measurements of the relative change of the amplitude of the TA signal with the frequency of modulation and the relative phase shift of the TA signals are recommended. The theoretical curves of the $|U_2(r)/U_2(0)|$ versus the frequency of modulation are presented in Fig. 5.

Theoretical curves of the relative phase shift of the TA signals $U_2(r)$ and $U_2(0)$ versus the frequency of modulation are presented in Fig. 6.

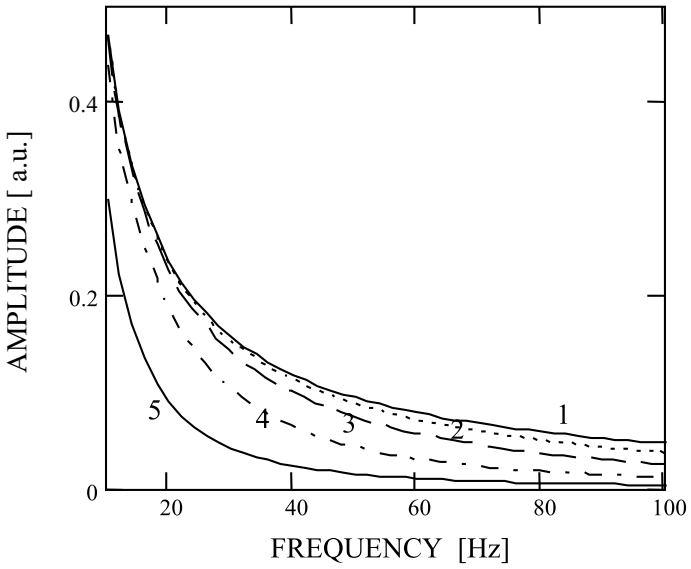

Fig. 3. Amplitudes of the TA signal versus the frequency of modulation for different values of the radius of the hole in the transistor packaging: Lines: 1) r = 500 μm (open transistor), 2) $r = 60$ μm, 3) $r = 50$ μm, 4) $r = 40$ μm, 5) $r = 30$ μm.

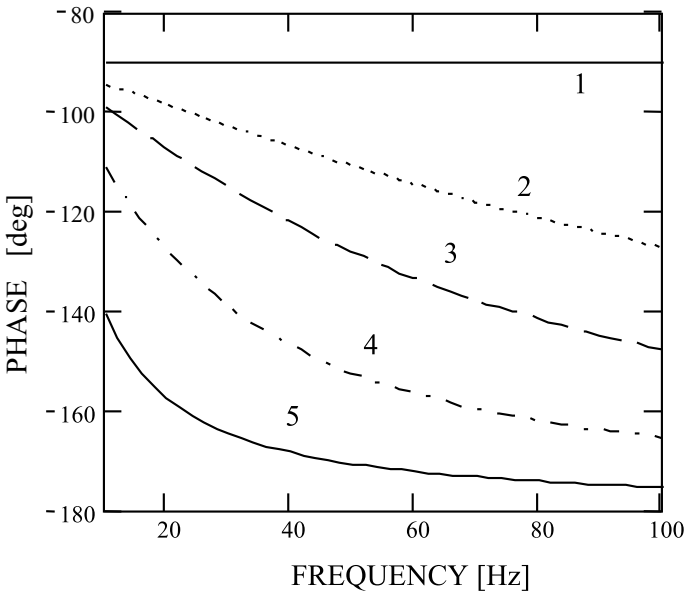

Fig. 4. Phases of the TA signal versus frequency of modulation for different values of a radius of the hole. Lines: 1) r = 500 μm (open transistor), 2) r = 60 μm, 3) r = 50 μm, 4) r = 40 μm, 5) $r = 30$ μm.

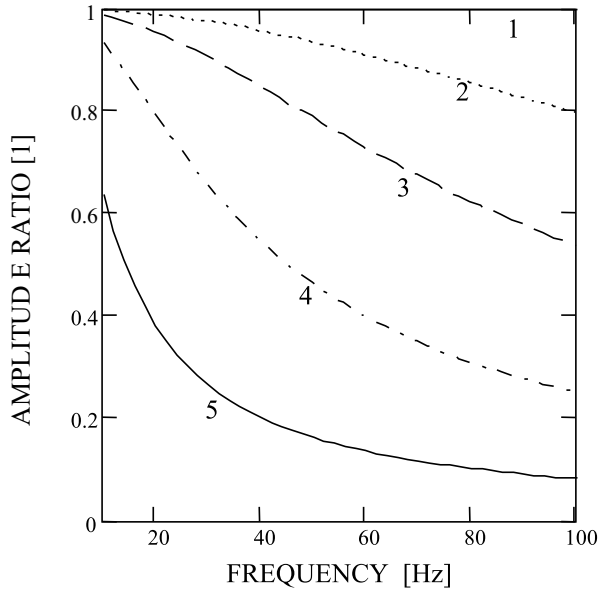

Fig. 5. Ratio of the amplitudes $|U_2(r)/U_2(0)|$ of the thermoacoustic signals versus the frequency of modulation for different values of the radius of the hole: 1) $r = 500$ μm (open transistor), 2) r = 60 μm, 3) $r = 50$ μm, 4) r = 40μm, 5) r = 30 μm.

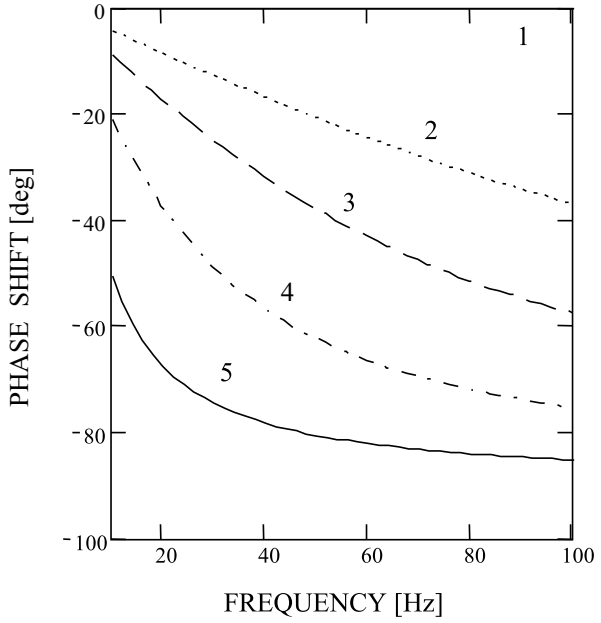

Fig. 6. Relative phase shifts of the thermoacoustic signals $U_2(r)$ and $U_2(0)$ versus the frequency of modulation for different values of the radius of the hole: 1) $r = 500$ μm (open transistor), 2) $r = 60$ μm, 3) $r = 50$ μm, 4) $r = 40$ μm, 5) $r = 30$ μm.

The electric model enables also the analysis of the dependences of the amplitude ratio of the TA signals on the radius of the hole for a series of modulation frequencies. The theoretical curves are presented in Fig. 7.

The dependences of the phase shift of TA signals on the radius of the hole for a series of modulation frequencies are presented in Fig. 8.

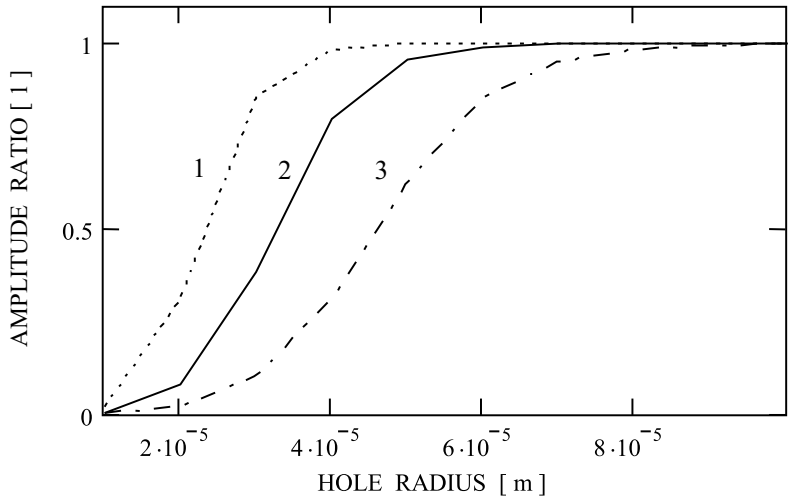

Fig. 7. Dependence of the amplitude ratio $|U_2(r)/U_2(0)|$ on the radius of the hole for three frequencies of modulation. Description of lines: 1) $f = 5$ Hz, 2) $f = 20$ Hz, 3) $f = 80$ Hz.

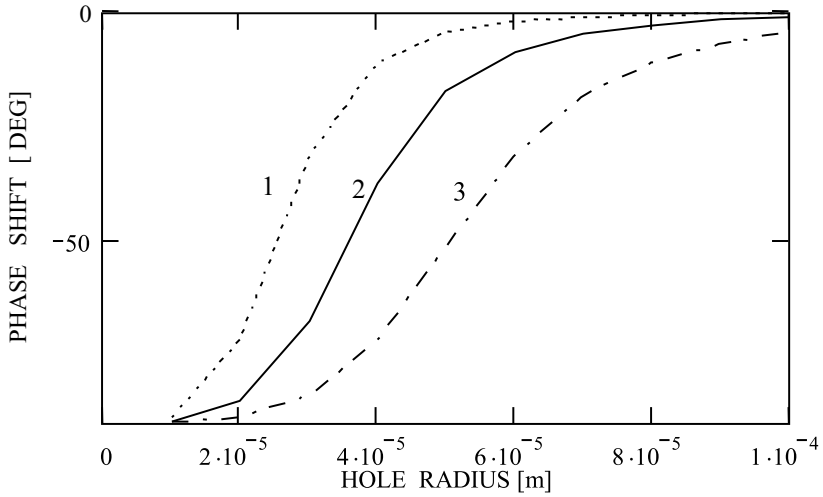

Fig. 8. Dependence of the relative phase shift of the thermoacoustic signals $U_2(r)$ and $U_2(0)$ on the radius of the hole for three frequencies of modulation. Description of lines: 1) $f = 5$ Hz, 2) $f = 20$ Hz, 3) $f = 80$ Hz.

3. Experimental results

Transistors in the common collector circuits were supplied with the constant voltage $U_{CE} = 15$ V and their collector currents I_C were controlled with a sinusoidal voltage generator in the base-emitter circuit U_{BE}. Collector currents were periodically modulated in the range $I_C = 10$ mA – 0 mA so that the maximum instantaneous electric power dissipated in the transistor was $P = 150$ mW. Thermoacoustic signals in the thermoacoustic chamber were detected by the electret microphone with a preamplifier. For the maximum power $P = 150$ mW and the frequency of modulation $f = 20$ Hz, the amplitude of the thermoacoustic signal was $U_2 = 200$ mV for an open transistor while for a closed transistor in the same conditions $U_2 = 0.0$ mV. The phase was measured between the TA signal and the voltage on the emitter resistor U_{RE} proportional to the collector current I_C. It was measured both with a digital oscilloscope and the electronic phase-meter. Amplitude of a TA signal was also measured with the digital oscilloscope and after the rectifier – with a digital multimeter.

For the purpose of testing of the proposed model, holes were done mechanically in the metal packagings of several transistors and a correlation between the theoretical model and experimental results was investigated.

Fittings of theoretical amplitude and phase curves to experimental results, obtained for the packaging TO39 of transistors BF178, are shown in Figs. 9 and 10 respectively.

Fitting of theoretical curves of the amplitude ratio and phase shift to experimental characteristics obtained for two other transistors is presented in Figs. 11 and 12 respectively.

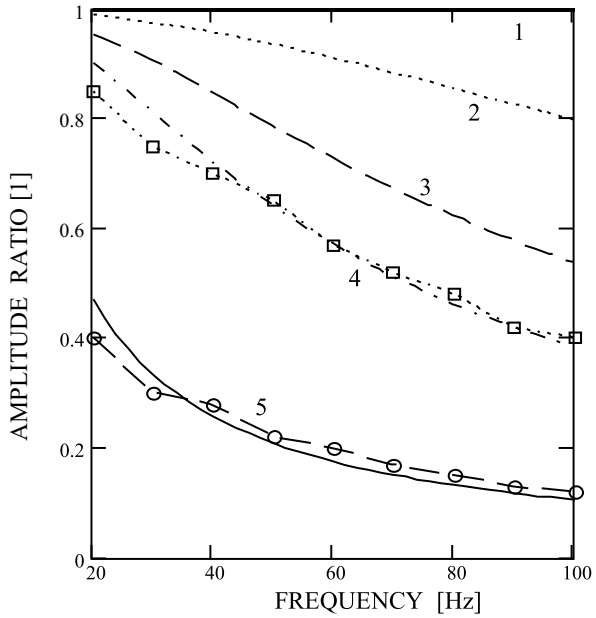

Fig. 9. Fitting of theoretical curves of the amplitude ratio to experimental results obtained for two transistors exhibiting different values of the radius of holes. Description of lines: 1) – open transistor, 2) r = 60 μm, 3) r = 50 μm, 4) r = 42 μm, 5) r = 32 μm.

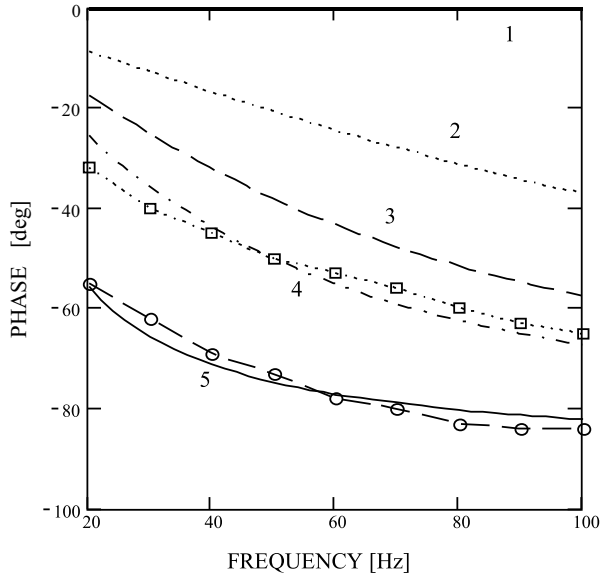

Fig. 10. Fitting of theoretical curves of the relative phase shift to experimental results obtained for two transistors exhibiting different values of the radius of holes. Description of lines: 1) – open transistor, 2) r = 60 μm, 3) r = 50 μm, 4) r= 45 μm, 5) r = 34 μm.

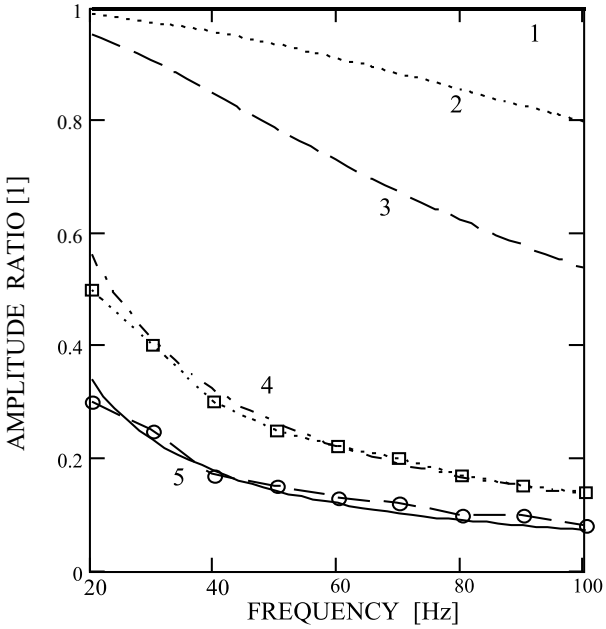

Fig. 11. Fitting of theoretical curves of the amplitude ratio to experimental results obtained for two transistors exhibiting different values of the radius of holes. Description of lines: 1) – open transistor, 2) r = 60 μm, 3) r = 50 μm, 4) r = 34 μm, 5) r = 29 μm.

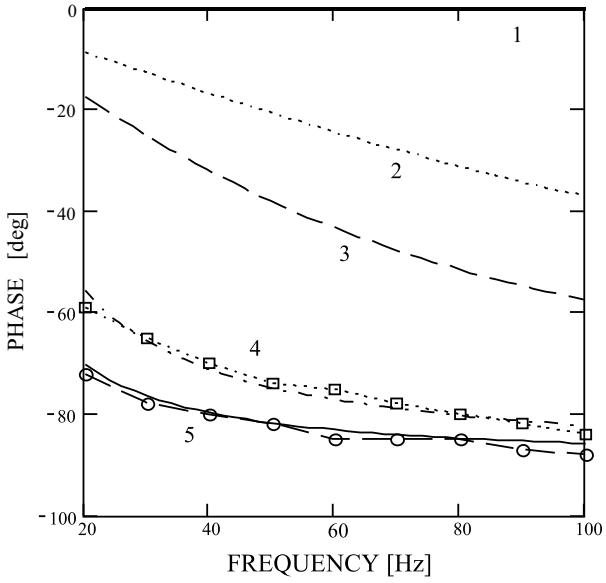

Fig. 12. Fitting of theoretical curves of the amplitude ratio to experimental results obtained for two transistors exhibiting different values of the radius of holes. Description of lines: 1) – open transistor, 2) r = 60 μm, 3) r = 50 μm, 4) r = 34 μm, 5) r = 29 μm.

4. Conclusions

The results of investigations of the correlation of the amplitude and phase thermoacoustic characteristics obtained for a series of transistor samples, exhibiting holes in the packaging, indicate that it is possible to determine the air tightness of packagings of electronic devices by this method. The measurements also present information about the sensitivity of this thermoacoustic approach. A good correlation of experimental results and theoretical characteristics, concerning both amplitude and phase, proves the correctness of the presented electric model of gas flow from the packaging to the thermoacoustic chamber.

References

[1] International Standard IEC 68-2-17.

[2] Polish Standard PN-878/E-04615.

[3] American Military Standard MIL-STD-202G.

[4] ARNOLD H. D., CRANDALL I. B., *Thermophone as a precision source of sound*, Phys. Rev., **10**, 22–38 (1917).

[5] ROSENCWAIG A., GERSHO A., *Theory of the photoacoustic effect with solids*, Journal of Applied Physics, **47**, 1, 64–69 (1976).

[6] HU H., WANG X., *Generalized theory of the photoacoustic effect in a multiplayer material*, Journal of Applied Physics, **86**, 7, 3953–3958 (1999).

[7] SUSZYŃSKI Z., *Photoacoustic diagnostic of the power transistors encapsulation*, Proc. XLIV Open Acoustic Seminar, 631–636, 1997.

[8] SUSZYŃSKI Z., *Quality investigation of adhesion of plastic encapsulant to the lead frame*, Proc. 10-th ICPPP Conf. Rome 194–196, 1999.

[9] BODERMAN A., *Photothermal defects in high power laser coatings at the limits of detection*, Progress in Natural Science, Supp. to **6**, 185–188 (1996).

[10] ROSENCWAIG A., OPSAL J., *Thermal wave imaging with thermoacoustic detection*, IEEE Trans. On Ultrasonic and Frequency Control UFFC-**33**, 5, 516–527 (1986).

[11] MALIŃSKI M., SUSZYŃSKI Z., BYCHTO L., *Determination of the quality of the soldering of semiconductor chips by the alternating-heat-flux method*, Micr. Journal, **29**, 209–213 (1998).

[12] MALIŃSKI M., SUSZYŃSKI Z., BYCHTO L., *Determination of the quality of the soldering of semiconductor chips by the thermal wave method*, 2-nd Therminic Workshop, 163–165 Budapest 1999.

[13] MALIŃSKI M., *Photoacoustics and photoacoustic spectroscopy of semiconductor materials*, TU of Koszalin, 2004.